

CONTROL SYSTEMS DEVELOPMENT DIVISION  
INTERNAL NOTE 74-EG-31

NASA CR-

141764

MULTI-MODE OPTICAL SENSOR (B)  
EVALUATION TEST REPORT

(NASA-CR-141764) MULTI-MODE OPTICAL SENSOR  
(B) EVALUATION TEST REPORT (Lockheed  
Electronics Co.) 53 p HC \$4.25 CSDL 20P

N75-22122

Unclas  
63/74 20084



DISTRIBUTION AND REFERENCING

*This paper is not suitable for general distribution or referencing. It may be referenced only in other working correspondence and documents by participating organizations.*



**National Aeronautics and Space Administration**  
**LYNDON B. JOHNSON SPACE CENTER**

**Houston, Texas**

January 3, 1975

LEC-5187  
SHUTTLE


CONTROL SYSTEMS DEVELOPMENT DIVISION  
INTERNAL NOTE 74-EG-31

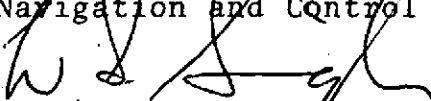
MULTI-MODE OPTICAL SENSOR (B)  
EVALUATION TEST REPORT


PREPARED BY

  
R. A. Smith, Principal Engineer  
Lockheed Electronics Company, Inc.

APPROVED BY

  
C. E. Manry, Laboratory Monitor  
Navigation and Control Branch

  
W. L. Swingle, Chief  
Navigation and Control Branch

  
Robert G. Chilton, Chief  
Control Systems Development Division

NATIONAL AERONAUTICS AND SPACE ADMINISTRATION  
LYNDON B. JOHNSON SPACE CENTER  
HOUSTON, TEXAS

January 1975

LEC-5187  
SHUTTLE

## ABSTRACT

The second engineering model of the Multi-Mode Optical Sensor (MMOS-B) was delivered in July 1973 by ITT/Gilfillan. An evaluation test series was performed on the unit in order to develop realistic specifications for a similar device for use on the Orbiter vehicle. Tests included sensitivity, target dynamic range, tracking angular rate, external magnetic field effects, and photocathode uniformity. Also, several demonstrations of operation under automatic control were prepared, using a desk calculator for numerical control and subsequent reduction of data derived from the test.

## ACKNOWLEDGEMENTS

This document was prepared by Lockheed Electronics Company, Inc., Aerospace Systems Division, Houston, Texas, for the Control Systems Development Division at the Lyndon B. Johnson Space Center (JSC) under Contract NAS 9-12200, Job Order 35-459. It was written by Robert A. Smith, Principal Engineer, and approved by James M. Lecher, Supervisor of the Guidance Systems Section, and William R. Labby, Manager of Guidance, Control and Instrumentation Department, Lockheed Electronics Company, Inc.

## CONTENTS

Section		Page
1.0	INTRODUCTION . . . . .	1-1
2.0	SENSOR DESCRIPTION . . . . .	2-1
2.1	Physical Parameters . . . . .	2-1
2.2	Operational Parameters. . . . .	2-1
2.2.1	Full-field acquisition and tracking mode (star and beacon targets) . . . . .	2-6
2.2.2	Acquisition and tracking of a designated target by external control mode . . . . .	2-7
2.2.3	Horizon profile radiometer mode . . . . .	2-8
2.2.4	Extended-target-tracking mode . . . . .	2-9
2.2.5	Lo-map mode. . . . .	2-9
2.2.6	Hi-map mode. . . . .	2-9
2.2.7	Landmark-tracking mode . . . . .	2-9
3.0	TEST INSTRUMENTATION AND FACILITIES. . . . .	3-1
3.1	Calculator Control Unit (CCU) . . . . .	3-1
3.2	Manual Control Unit (MCU) . . . . .	3-2
3.3	Two-Star Simulator. . . . .	3-2
3.4	H. R. Moore Two-Axis Mounting Table . . . . .	3-3
3.5	Ultraviolet Horizon Simulator . . . . .	3-3
3.6	Beacon Simulator. . . . .	3-4
3.7	Star Field Simulator. . . . .	3-4

Section	Page
3.8 Video Display Device. . . . .	3-5
3.9 Rotary Table Device (ROTAB) . . . . .	3-5
4.0 TEST OBJECTIVES, PROCEDURES, AND RESULTS . .	4-1
4.1 Operational Test. . . . .	4-1
4.1.1 Objective. . . . .	4-1
4.1.2 Description. . . . .	4-1
4.1.3 Results. . . . .	4-1
4.1.4 Discussion . . . . .	4-2
4.2 Target Sensitivity. . . . .	4-2
4.2.1 Objective. . . . .	4-2
4.2.2 Procedure. . . . .	4-2
4.2.3 Results. . . . .	4-3
4.2.4 Discussion . . . . .	4-3
4.3 Target Brightness Range . . . . .	4-4
4.3.1 Objective. . . . .	4-4
4.3.2 Procedure. . . . .	4-4
4.3.3 Results. . . . .	4-4
4.3.4 Discussion . . . . .	4-5
4.4 Tracking Rate . . . . .	4-6
4.4.1 Objective. . . . .	4-6
4.4.2 Procedure. . . . .	4-6
4.4.3 Results. . . . .	4-6
4.4.4 Discussion . . . . .	4-10

Section	Page
4.5 Magnetic Field Susceptibility . . . . .	4-10
4.5.1 Objective. . . . .	4-10
4.5.2 Procedure. . . . .	4-10
4.5.3 Results. . . . .	4-11
4.5.4 Discussion . . . . .	4-11
4.6 False Target Recognition and Rejection Test. . . . .	4-12
4.6.1 Objective. . . . .	4-12
4.6.2 Procedure. . . . .	4-12
4.6.3 Results. . . . .	4-13
4.6.4 Discussion . . . . .	4-13
4.7 Photocathode Uniformity . . . . .	4-13
4.7.1 Objective. . . . .	4-13
4.7.2 Procedure. . . . .	4-14
4.7.3 Results. . . . .	4-14
4.7.4 Discussion . . . . .	4-14
4.8 Automatic Field Map . . . . .	4-16
4.8.1 Objective. . . . .	4-16
4.8.2 Procedure. . . . .	4-16
4.8.3 Results. . . . .	4-17
4.8.4 Discussion . . . . .	4-17

Section		Page
5.0	CONCLUSIONS. . . . .	5-1
5.1	Specific Conclusions. . . . .	5-1
5.1.1	Operational test (par 4.1) . . .	5-1
5.1.2	Target sensitivity (par 4.2) . .	5-1
5.1.3	Target brightness range (par 4.3). . . . .	5-2
5.1.4	Tracking rate (par 4.4). . . . .	5-2
5.1.5	Magnetic field susceptibility. .	5-2
5.1.6	False target recognition and rejection test (par 4.6) . . . .	5-3
5.1.7	Photocathode uniformity (par 4.7). . . . .	5-3
5.1.8	Automatic field map (par 4.8). .	5-4



# TABLES

Table		Page
I	MMOS OUTPUT AND INPUT LISTING . . . . .	2-3
II	POINT-TO-POINT SCALE FACTOR . . . . .	4-8
III	PHOTOCATHODE UNIFORMITY . . . . .	4-15
IV	FIELD MAP TEST DATA . . . . .	4-22

## FIGURES

Figure		Page
1	Multi-Mode Optical Sensor (MMOS-B) . . . . .	2-2
2	Rate test configuration. . . . .	4-7
3	Point-to-point scale factor. . . . .	4-9
4	A sample 37-point field map. . . . .	4-19
5	Sample 121-point field map . . . . .	4-21

## 1.0 INTRODUCTION

This document describes a particular series of evaluation tests which were done with the Phase B Multi-Mode Optical Sensor (MMOS-B).

The first MMOS was procured under Contract NAS 9-11934 from ITT Aerospace/Optical Division, and delivery of the engineering prototype model took place in March 1972. This unit did not have full provision for rendezvous tracking; however, its design characteristics permitted a subsequent modification program to include the rendezvous mode. The first model MMOS provided the following functional modes of operation:

- Full-field acquisition of the brightest star
- Star tracking
- Offset mode
- Ultraviolet horizon profile radiometer mode.

In December 1971, the basic contract NAS 9-11934 was extended to provide a Phase B portion of the MMOS program. The contract extension required delivery of a new "B" model MMOS in May 1973. This second model (MMOS-B) has the same functional modes of the earlier unit and also provides:

- Beacon-tracking mode
- Extended-target-tracking mode
- Hi-map mode
- Lo-map mode
- Landmark-tracking mode

Development of the MMOS-B design was directed toward exploring the feasibility of providing a general-purpose optical sensor making full use of the flexibility inherent in the image dissector tube. The finished design demonstrated capabilities for applications such as ultra-violet horizon sensing, landmark tracking, slow-scan television, and modulated beacon discrimination and extended-target tracking for rendezvous, in addition to its basic function as a star tracker for alinement of the inertial measurement unit. As the Orbiter vehicle operational requirements became better defined, interest in the varied functions of the MMOS-B became limited to its application as a star tracker and as a sunlit-target tracker for rendezvous. Therefore, the test program was reduced to cover principally the operating modes required for the Orbiter application:

- Full-field acquisition of the brightest star
- Target star tracking
- Offset command mode

The other modes which the MMOS-B is capable of providing will be tested in subsequent programs to determine their usefulness in meeting any future Orbiter operational requirements that may develop.

## 2.0 SENSOR DESCRIPTION

The MMOS-B is an electro-optical instrument designed to alternately function as a star and object tracker that acquires and tracks point or extended radiative and reflective sources; as a scanning radiometer that measures the earth horizon ultraviolet radiance profile; as a star field or earth surface mapper; and as an earth landmark tracker. It uses an S-20 photo surface image dissector as a primary sensor and does not have mechanical devices for spatial scanning purposes. However, it does employ rotary solenoids and detent motors for protective sun shutter and optical filter operations.

### 2.1 Physical Parameters

The MMOS-B is entirely contained within a cylindrical package approximately 15 inches long and 6 inches in diameter. (See fig. 1.) All electrical connections are made through a cable connector located on one end of the instrument. The opposite end includes the optical lens and sunshade. The cylinder has no protuberances and is not constructed to be mounted in a specific position. The primary restraint to consider in mounting the sensor is the orientation of the tracker axes, which are defined by a two-surface alinement prism on the front of the instrument.

### 2.2 Operational Parameters

The MMOS-B incorporates seven primary modes of operation as follows:

- Full-field acquisition and tracking of the



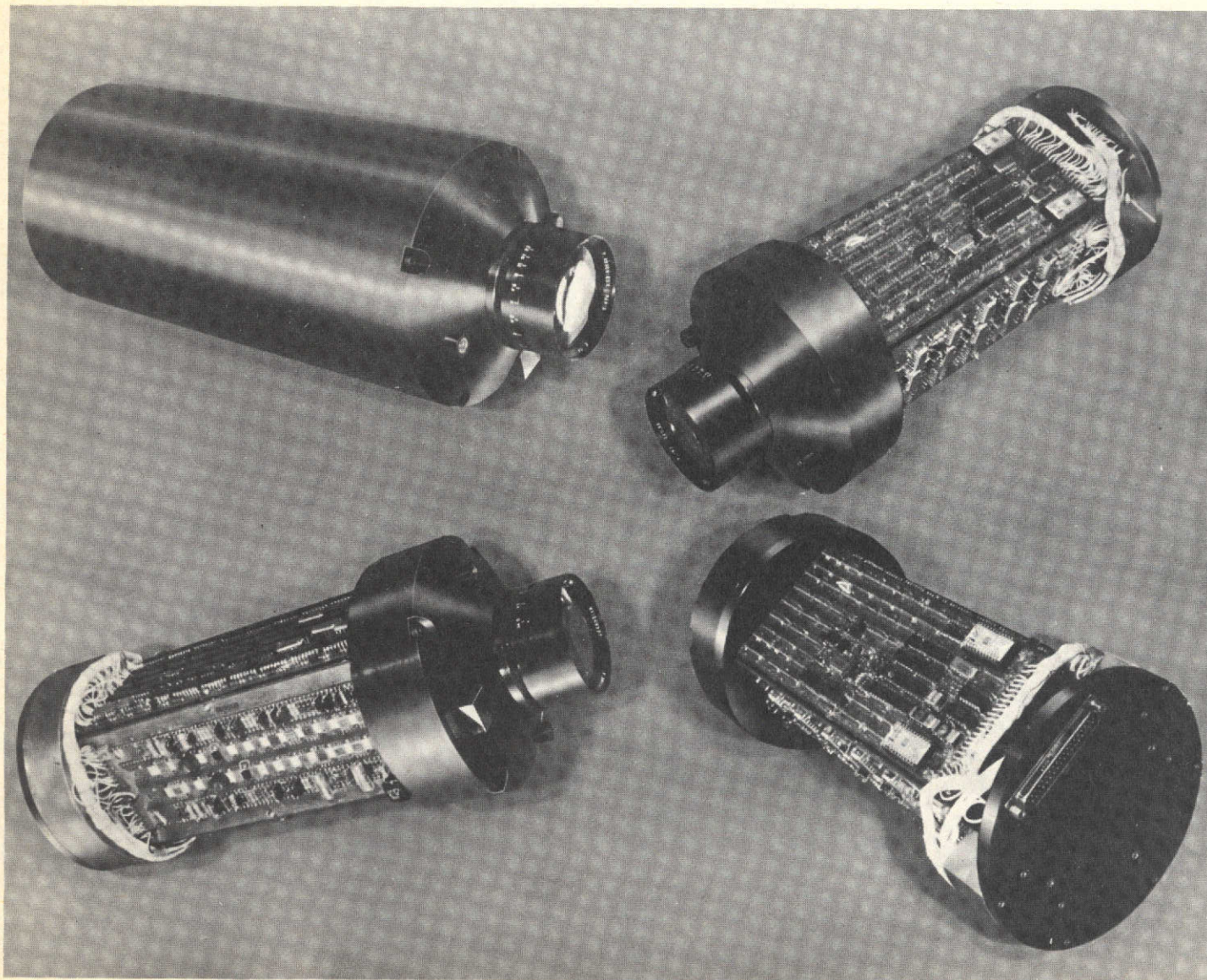


Figure 1. - Multi-Mode Optical Sensor (MMOS-B).

brightest star or beacon

- Acquisition and tracking of star or beacon designated by external control
- Horizon profile radiometer mode
- Extended-target-tracking mode
- Lo-map mode
- Hi-map mode
- Landmark-tracking mode

The sensor connector socket has numerous input and output points that may be used to externally control the unit, monitor mode status, and obtain data outputs. These points are listed below for reference and an aid to understanding the MMOS operation as outlined in subsequent paragraphs.

TABLE I. — MMOS OUTPUT AND INPUT LISTING

<u>Output</u>	<u>Description</u>
X-position error	±5 Vdc, 1 V/deg, target relative to boresight point, corrected for linearity, filtered to 5-Hz bandwidth. Data good only when sensor is tracking a target.
Y-position error	±5 Vdc, 1 V/deg, target relative to boresight point, corrected for linearity, filtered to 5-Hz bandwidth. Data good only when sensor is tracking a target.

<u>Output</u>	<u>Description</u>
X-position angle	±5 Vdc, 1 V/deg angular target scan position relative to boresight point. Scan position continuously valid.
Y-position angle	±5 Vdc, 1 V/deg angular target scan position relative to boresight point. Scan position continuously valid. Also used as horizon radiometer scan position.
Horizon intensity	0 to +5 Vdc, 5 Vdc level indicates radiance of $1.505 \times 10^{-2} \text{ W cm}^{-2} \text{ ster}^{-1} \text{ micron}^{-1}$ bandwidth $200 \text{ Å}$ centered at $3,850 \text{ Å}$ , 0 V. Zero dc level indicates zero radiance.
Target magnitude	0 to +5 Vdc (magnitude scale/volt determined during acceptance tests).
Target presence	+5 Vdc ±0.5 V level indicates a target is being tracked; 0 to 0.5 V exists when no target is being tracked.
Beacon presence	+5 Vdc ±0.5-V level indicates that the <i>tracked</i> target is modulated at 4.725-kHz; 0-V to 0.5-V level exists when the target is not modulated at the specified frequency.
Sun shutter position	Status of the sun shutter position. A +5 Vdc level indicates shutter closed with zero level for shutter open.
Video	Analog signals proportional to radiance level of target area being



<u>Output</u>	<u>Description</u>
	scanned. High and low level outputs are provided in separate channels.
Status Indicators	<p>TTL Logic</p> <p>Logic "1" = <math>3.5\text{ V} \pm 0.5\text{ V}</math> indicates operating mode.</p> <p>Logic "0" = <math>0\text{ V} \pm 0.5\text{ V}</math> indicates nonoperating mode.</p> <ol style="list-style-type: none"> <li>1. Acquisition mode</li> <li>2. Reacquisition mode</li> <li>3. Tracking mode</li> <li>4. Radiometer mode</li> <li>5. Lo-Map mode</li> <li>6. Hi-map mode</li> <li>7. X-target mode</li> <li>8. Landmark-tracking mode</li> <li>9. Low-gain condition</li> <li>10. Aperture position</li> <li>11. Attenuator condition</li> <li>12. UV filter</li> </ol>
X-position offset	$\pm 5\text{ Vdc}$ , 1 V/deg offset reacquisition scan field position relative to tracker boresight.
Y-position offset	$\pm 5\text{ Vdc}$ , 1 V/deg offset reacquisition scan field position relative to tracker boresight.

<u>Output</u>	<u>Description</u>
Command modes	Input of +5 Vdc 10 mA commands MMOS-B to desired modes.
	1. Lo-map
	2. Hi-map
	3. Offset
	4. Radiometer
	5. Extended target
	6. Landmark target

#### COMMAND RULES

1. The sensor is in the full automatic acquisition/track mode when there is no command signal applied.
2. Only one command signal is honored by the sensor logic. Switch to another mode will not take place until the original command is removed.
3. In the offset mode, if no target is acquired at the designated point, the command level must be removed before another mode command or offset designation can be made.

2.2.1 Full-field acquisition and tracking mode (star and beacon targets). The sensor is normally operating in this mode unless any of the other directive signals are present on the external command circuits.

The automatic acquisition/track sequence operates as follows: After the tracker turns on, the system goes to

the full-field acquisition state and begins a digital search pattern for a target star. As the scan progresses through the field, targets seen are observed in position and brightness, and at the end of one full-field scan sequence, the system directs the reacquisition field scan center to the position of the brightest star seen and verifies its presence. If the star is found, the sensor automatically switches to a track scan mode. If no target is found, the system switches back to the acquisition scan mode and repeats the cycle. When the switch to track mode is made and the target is found and tracked, a voltage appears on the "target presence" output pin and analog voltages denoting the X- and Y-field positions of the target appear on the correct output connector pins. If the target energy contains a 4.725-kHz modulation component, then a voltage also appears on the "beacon presence" output point.

If the target is lost, the system switches to the reacquisition mode ("mini-scan"), the target presence signal disappears, and the voltages on the XY-position error output terminals are not valid. The sensor searches the field area where the target was last seen for about 15 milliseconds, and if the target is not relocated, it switches back to full-field acquisition and starts a new search pattern. If the target is found in the reacquisition mode, the system switches to track, a *target presence* signal returns, and valid position error voltages are again present.

2.2.2 Acquisition and tracking of a designated target by external control mode. The sensor switches to this mode upon external command and positions the center of the

reacquisition field to a point in the field-of-view, which is determined by the analog voltage levels applied to the offset terminals.

If a target is seen by the reacquisition scan, the sensor switches to the track mode, shows *target presence*, and develops position voltage data. If no target is seen, the unit will remain in the "mini-scan" until allowed to return to automatic mode or until another series of offset voltages are applied and the sensor is again commanded to search.

2.2.3 Horizon profile radiometer mode. In this mode the sensor performs a function which is not related to the previously described acquisition/track operations.

When externally commanded, the sensor switches into a series of events which cause the instantaneous field of the dissector/optical system to be scanned in a vertical sweep through the total field-of-view without horizontal displacement. At the same time, a rotary solenoid inserts a 3,800 ( $\pm 100$  Å) filter into the optical path. The output circuitry provides a linear analog voltage which is proportional to the amount of radiant energy striking the particular photo cathode surface area defined by the translated instantaneous field-of-view. The scan is continuous at a 0.1-Hz rate until a mode change command is received by the sensor.

The instantaneous field-of-view position of the vertical scan is determined by monitoring the Y-position angle voltage output.

2.2.4 Extended-target-tracking mode. This method of operation is similar to the star track mode, except the cruciform scan pattern is lengthened to cover approximately  $6^\circ$ , peak-to-peak, in the field-of-view. No acquisition actions are taken, and when the MMOS-B is commanded to this mode, the enlarged track scan pattern is centered to the extended source target image. Target presence is then indicated and X- and Y-position error voltages are produced. If the target is lost, the system returns to the automatic mode.

2.2.5 Lo-map mode. In this mode the MMOS-B total field-of-view is continuously scanned at 8 frames/second. The same digital search pattern used in the automatic acquisition mode is used. X- and Y-position angle voltages appear at their proper output points, and voltage pulses proportional to target irradiance will be present at the video output. Stars as dim as +2.0 magnitude can be detected in this mode.

2.2.6 Hi-map mode. This mode is identical in operation and output characteristics to the lo-map mode. However, the sensitivity level is substantially lower than that of the lo-map mode. Scene brightnesses as high as 10,000 foot-lamberts (e.g., sunlit clouds) can be viewed safely in this mode.

2.2.7 Landmark-tracking mode. The landmark-tracking mode operates in a similar manner to the previously described map modes. The scan pattern is limited to a square field of  $2.5^\circ$ , and the digital search pattern is repeated at a 30 frames/second rate. X- and Y-position angle voltages

are present at the output, and video voltages proportional to the target irradiance are also available. The upper left-hand corner of the field position is determined by voltages present on the offset input lines, and is updated to these voltages once each frame.

### 3.0 TEST INSTRUMENTATION AND FACILITIES

The MMOS-B evaluation program tests have been conducted at JSC using the optical laboratory facilities in Building 16A. To adequately perform the tests, several items of special-purpose test equipment have been originally designed and constructed while other test equipment items result from modification of devices that have been used on previous JSC programs. These are explained in more detail in the following paragraphs.

#### 3.1 Calculator Control Unit (CCU)

A star tracker for the Orbiter will be operated by the onboard computer system for remote control, status monitoring, and data reduction. To make the evaluation program as realistic as possible to the intended future-use conditions, a method of control of the MMOS-B has been designed using the 9100B Hewlett-Packard desk calculator and associated interface equipment. The necessary components to effect the interface control operations are mounted in a portable rack cabinet that is designated as the Calculator Control Unit (CCU). Included in the cabinet are:

- Hewlett-Packard 2570A coupler/controller
- A control panel
- Power supplies for the MMOS-B input and logic control circuits
- D/A converters (for offset mode)
- A/D converters (for XY-position error, horizon radiance level, radiometer Y-axis position angle, and star magnitude inputs).

Complete control of the MMOS-B along with mode status, data reduction/smoothing, and printed readout of data points is possible with the CCU and calculator when properly connected to the MMOS-B via the single cable normally required to activate the instrument.

### 3.2 Manual Control Unit (MCU)

A secondary control unit that provides for manual mode selection, mode status signals, and adequate test points to permit initial setup, troubleshooting or inspection of signals being transferred from the MMOS-B to the CCU during normal operating functions has also been provided.

Included in the MCU cabinet are:

- Tektronix model 604 display monitor
- Hewlett-Packard 3440A digital voltmeter
- Control and indicator panel
- Test point panel
- Simulator panel
- Power supplies

The MCU can be used alone or with the CCU if monitoring or manual controls are needed for testing.

### 3.3 Two-Star Simulator

A Two-Star Simulator unit designed and fabricated by the Farrand Optical Company under Contract NAS 9-6064, June 8, 1966, was used to provide star targets for some tests.



This device provides two stars with separately variable magnitudes and is designed so that the collimated beams representing the two stars can be superposed at a point 40 feet from the instrument.

The star magnitude range is from -1.5 to +3.0  $M_V$  on one star, and +3.0 to +5.0  $M_V$  on the other. The angular separation can be continuously adjusted from superposition to 2° separation. The target output approximates a G2 spectral class star.

### 3.4 H. R. Moore Two-Axis Mounting Table

The H. R. Moore two-axis mounting table used to position the MMOS to a designated azimuth (X) and elevation (Y) pointing angle for certain test configurations. The table was calibrated to provide a precise pointing capability of 2 arc seconds and an interpolative capability of 1 arc second.

### 3.5 Ultraviolet Horizon Simulator

This device produces an acceptable simulation of the earth's ultraviolet horizon profile as it would appear to an Orbiter-mounted unit while operating at an altitude of 300 nautical miles. It is mounted on the reverse side of the Moore two-axis table so that the MMOS-B looks directly into the output collimated beam when rotated 180° from the front position.

The simulator is designed to produce proper radiance values in the 3,800 ( $\pm 100$  Å) window, accepts various types of profile targets, and provides for radiance calibration.

The optical collimator and target size have been selected to provide a radiance volume that is compatible with the MMOS-B field-of-view for a 300 nautical mile orbit simulation.

### 3.6 Beacon Simulator

The Beacon Simulator is used to test the MMOS-B response to a modulated beacon source. The simulator energy source is a xenon-arc lamp that can be modulated at 4.725 kHz up to an 80-percent level. Range of the beacon to the MMOS-B is simulated by using a specially constructed optical attenuator. With this device vacuum ranges from 1 to 1,000 miles are simulated under laboratory conditions.

### 3.7 Star Field Simulator

The Star Field Simulator was designed and constructed to provide a variety of targets for the MMOS-B accuracy tests. The unit can provide full-field display star targets of any number, magnitude, and angular displacement (within the total field) desired for the test program. It can be used to replace the Moore table and Two-Star Simulator combination for field mapping, target acquisition, and discrimination tests. The device is constructed to permit interchangeability of target plates as required.

When the simulator was used with the MMOS-B and properly programmed, CCU complete field map data was completed in a few minutes. Target plates depicting various extended source targets were used to test the extended-target tracking mode.

### 3.8 Video Display Device

The video display device is a Tektronix Model 604 Display Monitor, which has been supplied with a long persistence P7 phosphor cathode-ray tube. During use, X- and Y-position angle voltages are supplied to the horizontal and vertical oscilloscope inputs, and the video output voltage is connected to the oscilloscope Z-input. The position of the star targets and their relative brightnesses are visually displayed.

### 3.9 Rotary Table Device (ROTAB)

A rotary table unit located in the Inertial Systems Laboratory was made available for the MMOS-B tests. This device has a large rotary plate which can be turned at a controlled rate. The position of the table is indicated by a digital read-out system accurate to at least 5 arc seconds. Rates of rotation from  $0.01^\circ$  per second to over  $0.5^\circ$  per second are available. With the MMOS-B mounted on the table so that the objective lens nodal point is over the axis of rotation, a fixed star target will simulate a constant angular rate movement to the tracker.

## 4.0 TEST OBJECTIVES, PROCEDURES, AND RESULTS

In order to meet the goals of the MMOS-B evaluation test program as outlined in section 1.0, the following tests were completed:

- Operational Test (4.1)
- Target Sensitivity (4.2)
- Target Brightness Range (4.3)
- Tracking Rate (4.4)
- Magnetic Field Susceptibility (4.5)
- False Target Recognition and Rejection Test (4.6)
- Photocathode Uniformity (4.7)
- Automatic Field Map (4.8)

### 4.1 Operational Test

4.1.1 Objective. To determine the operability of all MMOS-B functions, including mode switching, output levels, and mode status signals.

4.1.2 Description. The MMOS-B will be mounted on the Moore two-axis table and connected to the CCU. Targets will be generated by the star and horizon simulators; then the CCU will be cycled to produce each mode function. Status will be monitored and position data (where applicable) will be verified for correct values.

4.1.3 Results. Although no specific evaluation data results from this test, it is useful in providing a

knowledge that the MMOS-B is, or is not, operating in a normal manner.

4.1.4 Discussion. It was originally intended that this test would only be used to test the operability of the MMOS-B during the evaluation program. As the tests progressed certain unusual conditions and suspicions of improper operation of the MMOS-B occurred, and these baseline operational tests helped to determine the conditions encountered and aided in their solutions. As a result of this test technique, it became obvious that a standard test series and use of a test set or fixtures was required to verify the operation of the flight models.

## 4.2 Target Sensitivity

4.2.1 Objective. To observe the ability of the MMOS-B to acquire and track star targets of low intensity and to finally ascertain the threshold sensitivity to be expected during operational sequencing.

4.2.2 Procedure. The MMOS-B was placed on the Moore table with the Star Field Simulator used as the target source. Prior to placing the MMOS-B into position, the simulator calibration was verified with the Pritchard Photometer, and was then set to a +3  $M_v$  target brightness level. After placing the MMOS-B into position, the star was acquired and tracked by controlling the MMOS-B with the Manual Control Unit (MCU). The target magnitude voltage was read and recorded from the MCU panel digital voltmeter. The test was done by sequencing the MMOS-B to allow it to acquire the target star while in the automatic

mode. After tracking had begun, the target magnitude was noted and recorded. This event chain was then repeated for other star target brightness values as needed. The threshold level was determined by lowering the target brightness until the MMOS-B would not acquire. A secondary effect test was conducted to determine the loss of signal (LOS) point of the MMOS-B while it was in a tracking mode on a previously acquired target. The target brightness was lowered until the MMOS-B dropped out of track and went to the automatic mode.

4.2.3 Results. The following significant data was taken to illustrate the test objective:

<u>Target Magnitude (Volts)</u>	<u>Target Irradiance (S20 watts cm<sup>-2</sup>)</u>	<u>Target Brightness (Visual Magnitude)</u>
0.81	$2.89 \times 10^{-14}$	+3.00
*0.41	$1.72 \times 10^{-14}$	+3.79
**0.29	$1.22 \times 10^{-14}$	+4.06

\*MMOS-B failure to acquire level

\*\*Loss of signal level

Offset and automatic acquisition have the same threshold.

4.2.4 Discussion. The MMOS-B was designed to acquire and track star targets of +3.0 magnitude or brighter. The test demonstrates this capability, because at the level of +3.0 magnitude, the unit acquired and tracked the target 100 percent of the times tried. At the level of +3.79 magnitude, no acquisitions were made. In between these brightnesses, acquisition was spotty and it probably is possible to establish a useable track/no track ratio curve slope between the points.

It was also determined that the automatic acquisition and offset modes have equal thresholds. This is the effect which was anticipated for the tracker where no perceptible background radiation exists. Introduction of a background level will produce different threshold level values, depending upon the amount of background present. Loss of track at a target level below acquisition thresholds is an expected result of this type of unit due to the signal processing and logic techniques used in the MMOS-B basic design.

### 4.3 Target Brightness Range

4.3.1 Objective. To determine the ability of the MMOS-B to acquire and track star targets of different intensities, and to ascertain the target brightness range through which it will operate and supply accurate and dependable position data.

4.3.2 Procedure. The MMOS-B was placed on the Moore table with the Star Field Simulator used as the target source. The MMOS-B position was adjusted so that the center field star target was located on its electrical axis, (X,Y equal to 0,0). The target intensity was then cycled from  $+3 M_v$  to brighter values with target magnitude and X,Y position data taken and recorded.

4.3.3 Results. Position values recorded are a result of computing the average values of ten samples of error voltages taken at the X,Y position of 0,0 and of applying a one volt per degree scale factor to the results. Target brightness was varied from  $+3 M_v$  to  $-3 M_v$  and the following data was taken.

<u>Target Magnitude</u> <u>(Volts)</u>	<u>Visual</u> <u>Magnitude</u>	<u>X Pos</u>	<u>Y Pos</u> <u>(MV)</u>	<u>X Pos</u> <u>(sec)</u>	<u>Y Pos</u> <u>(sec)</u>
.81	3.0	2	3	7	11
1.18	2.5	1	2	4	7
1.66	2.0	2	2	7	7
2.21	1.5	3	2	11	7
2.78	1.0	1	3	4	11
3.35	0.5	2	2	7	7
3.80	0	0	3	0	11
4.25	-0.5	2	2	7	7
4.49	-1.0	3	4	11	14
4.64	-1.5	3	2	11	7
4.75	-2.0	2	4	7	14
4.76	-2.5	3	4	11	14
*1.23	-3.0	12	16	43	58

\*Attenuation automatically activated between -2.5 and -3.0 magnitudes.

4.3.4 Discussion. It can be seen from the test data that the MMOS-B has excellent positional data stability from the dim +3.0  $M_V$  to the point where the attenuation mechanism activates. A subsequent test performed after the data was taken indicated that the attenuator moved into position at  $\approx -2.8 M_V$ . At this time the shift in X and Y position indicated was caused by the attenuator aperture positioning in the optical system. Repeated cyclings indicated that the shift (approximately one arc minute), was constant and repeatable. From this test, it can be concluded that the method of attenuation used can cause positional data shifts, and therefore, further analysis of the process, optical or mechanical, needs to be considered in the design of subsequent star trackers.



## 4.4 Tracking Rate

4.4.1 Objective. To determine the error lag produced by the MMOS-B when tracking a target moving at constant velocities through the field of view.

4.4.2 Procedure. The MMOS-B was positioned on the ROTAB with the Star Field Simulator used to provide a stable single star target. (See fig. 2.) The alinement and mounting method for the MMOS-B was done in a manner which insured that, as the table turned, the target moved only in the X axis with a constant  $-0.5^\circ$  Y-axis displacement during the total X field of view traverse from  $-5^\circ$  through  $0^\circ$ , then to  $+5^\circ$ . Data was taken and recorded by means of the Calculator Control Unit (CCU), consisting of a reading of table position and X-axis error output voltage, which correlated to the star target position in the field of view. Table rotation rates were varied with data runs made at 0.1, 0.2, 0.3 and 0.5 degrees/second. In order to establish a scale factor measurement at various field positions, the table was slowed to 0.01 degrees/second and table position/X error output voltages were recorded. The data rate, which was dependent upon the HP9100B Calculator System, was approximately two points per second.

4.4.3 Results. From the data taken, the tracking lag was computed for each rate. The scale factor data came from the low rate (0.01 degrees/sec) calibration. Scale factor points were selected to be the values nearest the ROTAB position tabulations for the various rates. The lag errors at the selected rates are shown in table II and figure 3.

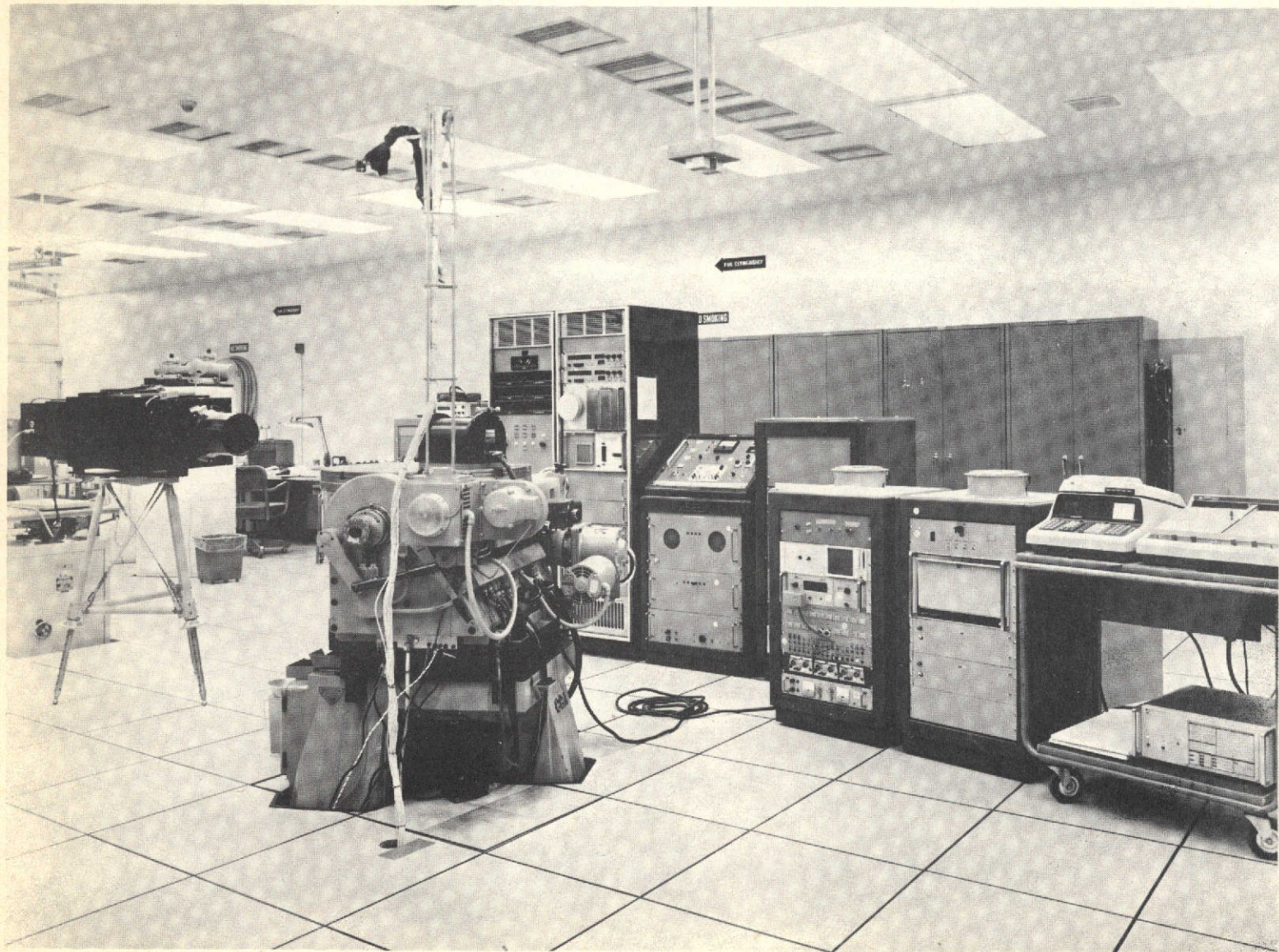


Figure 2. - Rate test configuration.

TABLE II. - POINT-TO-POINT SCALE FACTOR  
Lag (arc seconds)

<u>0.1 degrees/sec</u>	<u>0.2 degrees/sec</u>	<u>0.3 degrees/sec</u>	<u>0.5 degrees/sec</u>
46.30	63.91	106.74	184.60
53.40	74.60	99.40	184.78
39.14	56.70	117.42	170.02
35.45	74.50	99.36	178.40
31.87	63.55	139.27	
39.19	63.69		
31.90			
28.17			
39.05			
35.43			



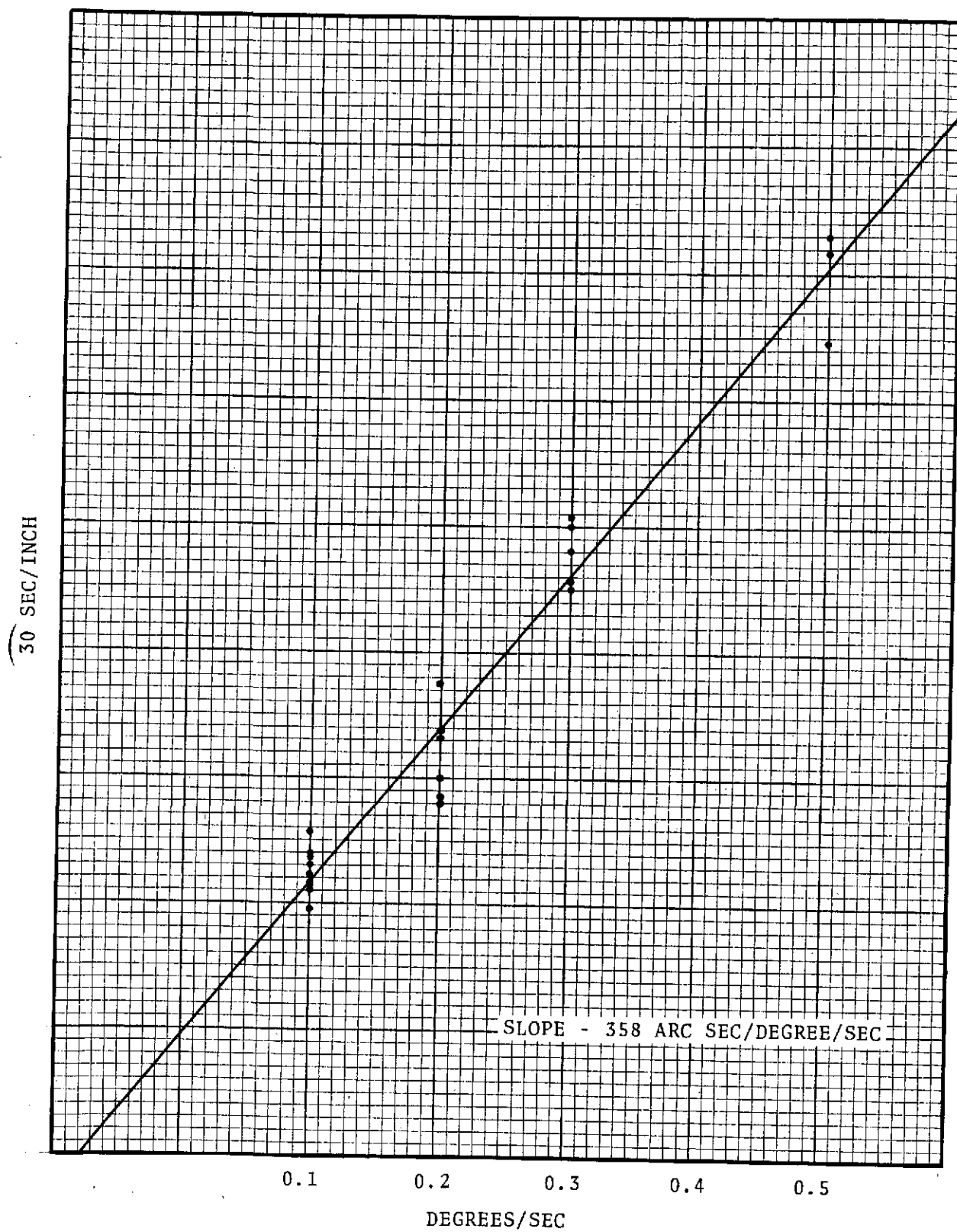


Figure 3. - Point-to-point scale factor.

4.4.4 Discussion. The MMOS-B performed in a predictable manner as regards the tracking lag values obtained. At 0.2 degrees/sec, the lag closely approaches the maximum acceptable pointing error of one arc minute and has a linear reaction to target velocity throughout the range tested. Although the higher rates increased the lag error, the tracker demonstrated the tenacity required to hold a target at the maximum rate tested.

#### 4.5 Magnetic Field Susceptibility

4.5.1 Objective. To determine the susceptibility of the MMOS-B to an external magnetic field, and to ascertain if there are any observable deleterious operational effects to be noted during the presence of the field.

4.5.2 Procedure. The MMOS-B was placed on a wooden platform in the center of the laboratory room so that any metallic objects were not closer than five feet. The unit was activated and the Star Simulator was used to provide a star target from a point in front of the MMOS-B. The magnetic field was supplied by passing a dc current through a single no. 12 conductor, which could be positioned parallel or perpendicular to the MMOS-B cylinder at any external distance up to touching the external shell. Measurement of the field generated was made with a Bell Model 120 Gaussmeter.

The star tracker was set to a  $+3 M_v$  level, and was then acquired and tracked by the MMOS-B while X and Y position data were recorded. The external conductor was placed parallel, perpendicular, and at various distances

and locations in relation to the MMOS-B outside shell. As the conductor was moved to new positions, the X and Y position voltages were observed for change.

4.5.3 Results. With the equipment available, it was possible to pass a current of 25 amperes through the conductor and by use of the Gaussmeter, a magnetic field of 5.2 to 5.5 gauss was measured at a point 1 cm from the wire. At this level, no perceptible change was noted in the X and Y output voltages for all positions of the conductor.

4.5.4 Discussion. From the results obtained in this particular test, it is obvious that the MMOS-B has adequate magnetic shielding to protect it from the induced field, which is somewhat greater than that of the earth. It should be noted that measurement of the flux density at the shell does not evaluate the total effect of an external field to the internal dissector/deflection assembly. It only shows that the magnetic shielding peculiar to the MMOS-B construction is adequate to cause the effect to be negligible for the conditions of this test. Subsequent tests using higher intensity fields are needed to properly evaluate the problem. A star tracker design should be made which would ensure that no significant effect on its accuracy would be present from any magnetic field environments experienced when it is used in the Orbiter under operational situations.

#### 4.6 False Target Recognition And Rejection Test

4.6.1 Objective. To develop and test a system for calculator control of the MMOS-B in order to provide a false target recognition and rejection technique.

4.6.2 Procedure. The MMOS-B was mounted on the Moore table and adjusted to observe the Farrand Two-Star Simulator for a fixed target. The star target intensity was adjusted to approximately  $+2 M_v$  brightness during the test. Another star target was supplied by using a pinhole and light source which was mounted on an arm secured to the shaft of a low speed electric motor. This source was adjusted to provide a brighter (approximately  $0 M_v$ ) target brightness. The motor speed and target position on the arm was set to provide a target movement of about  $0.25^\circ$  per second through the MMOS field with a circular movement diameter of near  $3.5^\circ$  in the field. The unit was positioned to insure that the fixed star target lay on the circumference of the rotating pattern, so that once during each revolution the targets were superposed.

A calculator program was generated which would control the MMOS-B and periodically monitor the X and Y position outputs while in the track mode. Subprogramming analyzed the X and Y positions for any detectable changes in the target position greater than error variations normally encountered by system noise during static track. If a change which exceeded the normal value was seen, the MMOS-B track was broken and the calculator established an offset mode to reestablish track on the original target position. This program continued without operator

attention until stopped or a new set of track/position parameters were established.

4.6.3 Results. The test was started and the fixed star was acquired and tracked by the MMOS-B. The rotating target was started, and it was observed that as superposition occurred, the MMOS-B changed targets and began to follow the brighter moving star. The calculator program was then started, and it was observed that shortly after the brighter movable star was acquired, the MMOS-B shifted to offset mode and reacquired the fixed target. The pattern repeated with the same sequence of events after each subsequent superposition.

4.6.4 Discussion. The test successfully demonstrates a way to provide discrimination between two targets and to finally select the desired target as determined by the parameters selected. It is an example of one condition that may be encountered on a space vehicle, if small sunlit particles of space debris or water crystals appear in a Star Tracker field of view and disturb the track operation. This method also illustrates the value of the offset mode in keeping the tracker under control and designating its target.

## 4.7 Photocathode Uniformity

4.7.1 Objective. To determine the sensitivity uniformity of the MMOS-B image dissector sensor photocathode at selected points through the operational field of view.



4.7.2 Procedure. The MMOS-B was placed on the Moore table with the Star Field Simulator used as the target source. The MMOS-B position was adjusted so that the center field star target was located on its electrical axis, (X,Y equal to 0,0). The target intensity was set to a +2  $M_V$  level for the test duration. The Moore table was then adjusted to all the desired star position values within the field of view and target magnitude values were recorded.

4.7.3 Results. The values of target magnitude obtained at the field points located at one degree intervals are tabulated in table III.

4.7.4 Discussion. From the target magnitude values obtained, it can readily be seen that the image dissector photocathode is not uniform. This condition will be true of any tube used in Shuttle star trackers, and therefore, must be considered in preparing operational specifications. The data on this tube shows a low sensitivity point in the upper +X corner of the field and a higher sensitivity buildup down the field diagonal to the lower -X position. A difference of 1.3 star magnitudes exists between the high and low points. This value represents a variance of 33 percent in photocathode sensitivity. Referring to the results of section 4.2, Target Sensitivity Tests, it can be predicted that an acquired target at XY coordinates of  $-5^\circ$ ,  $-5^\circ$  which measured to be +3  $M_V$  would probably not be acquireable at the XY point of  $5^\circ$ ,  $5^\circ$ , due to the loss in photocathode sensitivity which would give the target an apparent +4.3  $M_V$  value. The results of the test in section 4.2 show the threshold to be 0.79 magnitude below

TABLE III. - PHOTOCATHODE UNIFORMITY ( $M_V$ )

5	2.1	2.1	2.2	2.3	2.3	2.4	2.4	2.4	2.7	2.7	2.8
4	1.9	2.1	2.1	2.2	2.2	2.3	2.4	2.4	2.6	2.7	2.8
3	1.8	1.9	2.0	2.1	2.2	2.4	2.4	2.5	2.6	2.7	2.8
2	1.8	1.8	1.9	2.0	2.1	2.2	2.3	2.5	2.6	2.6	2.8
1	1.7	1.7	1.8	1.9	2.0	2.1	2.2	2.3	2.4	2.6	2.7
0	1.7	1.7	1.8	1.8	1.9	2.0	2.1	2.2	2.4	2.6	2.7
1	1.6	1.7	1.7	1.8	1.9	1.9	2.0	2.2	2.4	2.5	2.7
2	1.6	1.7	1.8	1.8	1.9	2.0	2.0	2.2	2.3	2.5	2.6
3	1.5	1.6	1.7	1.8	1.9	2.0	2.0	2.2	2.3	2.5	2.6
4	1.5	1.7	1.7	1.8	1.9	2.0	2.1	2.2	2.3	2.5	2.6
5	1.6	1.6	1.7	1.8	1.9	2.0	2.1	2.2	2.2	2.5	2.5
	5	4	3	2	1	0	1	2	3	4	5

$X^\circ$

specification level of +3 magnitude. This difference represents a value of 21 percent photocathode sensitivity variance, which would be the maximum allowable to insure acquisition of a +3  $M_V$  star in all portions of the field of view.

Experience with other image dissector sensors and discussions with tube manufacturers indicate that any other tube will probably have different sensitivity distributions. It is even possible to have a center dropoff with high response in the corners. What is important in specifying tube selection is to insure that the high and low sensitivity areas are as nearly uniform as possible regardless of area distribution. By tube selection processes, it will be possible to maintain an adequate variance of 15 to 20 percent. Lower values of variance may be achieved by checking a larger number of samples, but the cost/time factors of tube supply will escalate as the specification value is lowered.

#### 4.8 Automatic Field Map

4.8.1 Objective. To develop and test a system for calculator control of the MMOS-B to provide an automatic field map recording system which includes field positioning, data taking, position calculation, and plotting on recording of the finished product.

4.8.2 Procedure. The MMOS-B was placed on the Moore table with the Star Simulator placed in front of the table to supply the one degree separation field map targets. The HP Coupler/Calculator (CCU) was connected to the MMOS-B

and both Digital Printer and Calculator Plotter were readied to accept data and plot a completed map. The system was programmed to provide the following sequence of events:

1. Places correct position (X-Y) voltages on the offset input and commands the MMOS-B to offset mode.
2. Searches for and receives the target presence signal.
3. Selects data from X and Y error channel.
4. Performs averaging of positional data, and computes angle position by multiplication by the respective scale factor.
5. Plots the computed point position in respect to the absolute anticipated position.
6. Breaks MMOS-B track and repeats the process for the next point.

4.8.3 Results. The system was set up and performed satisfactorily. The ability to produce field maps with any pattern of star targets within the capability of the Star Simulator was demonstrated.

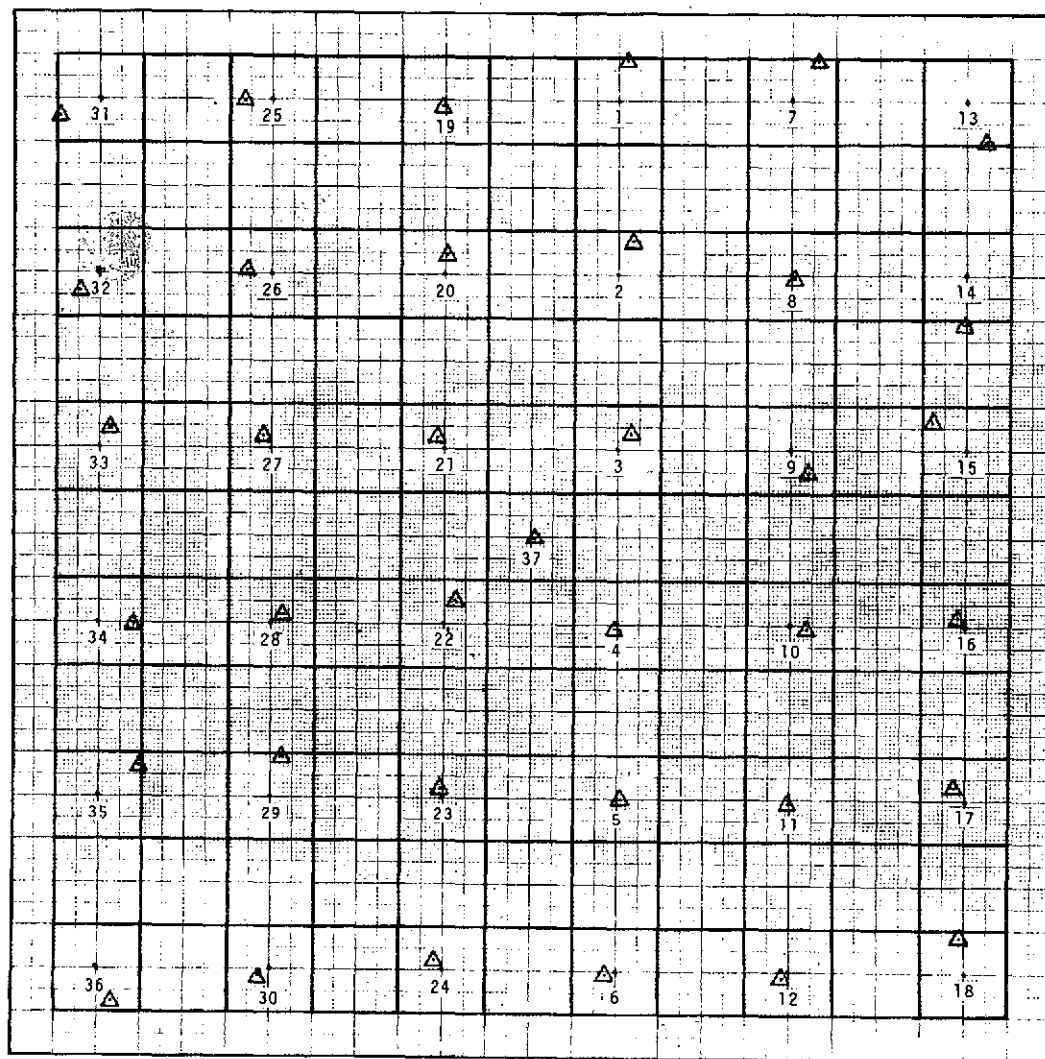
4.8.4 Discussion. The results of this test demonstrate the ability of the MMOS-B to be controlled and to supply usable data to a programmed calculator system. The substitution of a small computer to perform the same operations with even more operational programs, data storage, and problem calculations is an obvious conclusion to be made from the demonstration. The automatic operations and

correct reception to properly initiated external commands demonstrated by the MMOS-B can be included in a modified form in the Orbiter Star Tracker as desired, providing that Star Tracker/Computer interface logic rules are established in the overall system concept.

The offset mode control feature found in the MMOS-B was highly instrumental in the success of these tests. Although there are other methods of causing star target selection in the laboratory which would not require an offset mode, such a choice of target selection will not be available while the Orbiter is in flight and using real star targets. Therefore, the presence of an offset mode of operation appears mandatory to its successful employment.

A completed field map is useful for evaluation of performance, detection of problem or fault areas, and in developing improvements in design criteria. They can contain any number of target points with field of view locations which are limited by target simulator capabilities or by some acquisition limitations inherent to the Star Tracker.

A sample field map is shown in figure 4. This particular type has 36 targets equally spaced at the 1°, 3°, 5° points in the ten-degree field. Target number 37 is the field center and is used as the origin of the coordinate system. In order to boldly see the error values and the location of the actual plotted point (designated by the triangle), the area (black encircled square) immediately around the true position (single point designation) is scaled to  $\pm$  one arc minute. A line drawn from the true point to the actual point will illustrate the error in polar rotation, thereby



# FIELD MAP TEST

## DEVIATION (SEC)

DATA POINT	X	Y
1	13.2	59.3
2	22.4	47.1
3	18.5	21.8
4	(5.7)	(4.6)
5	3.9	0.4
6	(15.6)	(4.3)
7	36.3	60.7
8	2.8	(3.9)
9	24.9	(32.9)
10	23.1	(4.6)
11	(1.1)	(5.0)
12	(10.3)	(8.9)
13	28.4	(57.5)
14	(0.4)	(66.1)
15	(47.3)	38.2
16	(11.7)	12.5
17	(14.6)	18.9
18	(6.4)	50.0
19	(2.5)	7.1
20	3.2	27.5
21	(9.9)	14.6
22	14.9	32.5
23	(2.8)	13.2
24	(12.4)	13.6
25	(40.5)	(2.9)
26	(34.8)	5.0
27	(12.4)	17.8
28	15.3	12.9
29	14.9	55.3
30	(16.0)	(8.9)
31	(55.1)	(23.2)
32	(27.7)	(24.6)
33	9.6	(25.7)
34	49.8	(3.9)
35	57.6	42.5
36	20.9	(46.1)
37	0.9	0.1

Figure 4. - A sample 37-point field map.

showing at a glance the direction and magnitude of the error. The data supplied in the table shows the individual X and Y displacements in the arc seconds.

Another type of field map is shown by figure 5 and table IV. A group of 121 points are represented by targets spaced at each one-degree point in the entire ten-degree field. The error is shown by the vector method and the associated chart gives the errors in arc seconds for each point. This type of map is good for quick observation of an error shift or possible rotation about a point, and can be used to effectively determine if the field error pattern is changing when environmental temperature changes or mechanical stimuli are being applied. In this representation, the area around the point represents an expanded error scale as was done in the first type.

In order to make the field map effective for testing and evaluation, the data, which is eventually used to present the graphic map, must be taken quickly so that changes from external processes or environment will be minimal over the field. The automatic method described can fulfill the requirements needed for speed of measurement in order to provide reliable graphic field maps that can be used for test records, performance checking, and engineering development. It is an innovative achievement to take advantage of the automatic multi-mode capabilities of the MMOS-B that provide the basis for a Test Set concept to be used for subsequent Orbiter Star Tracker field operational checks and reverification of accuracy after flight or ground maintenance.

4-21

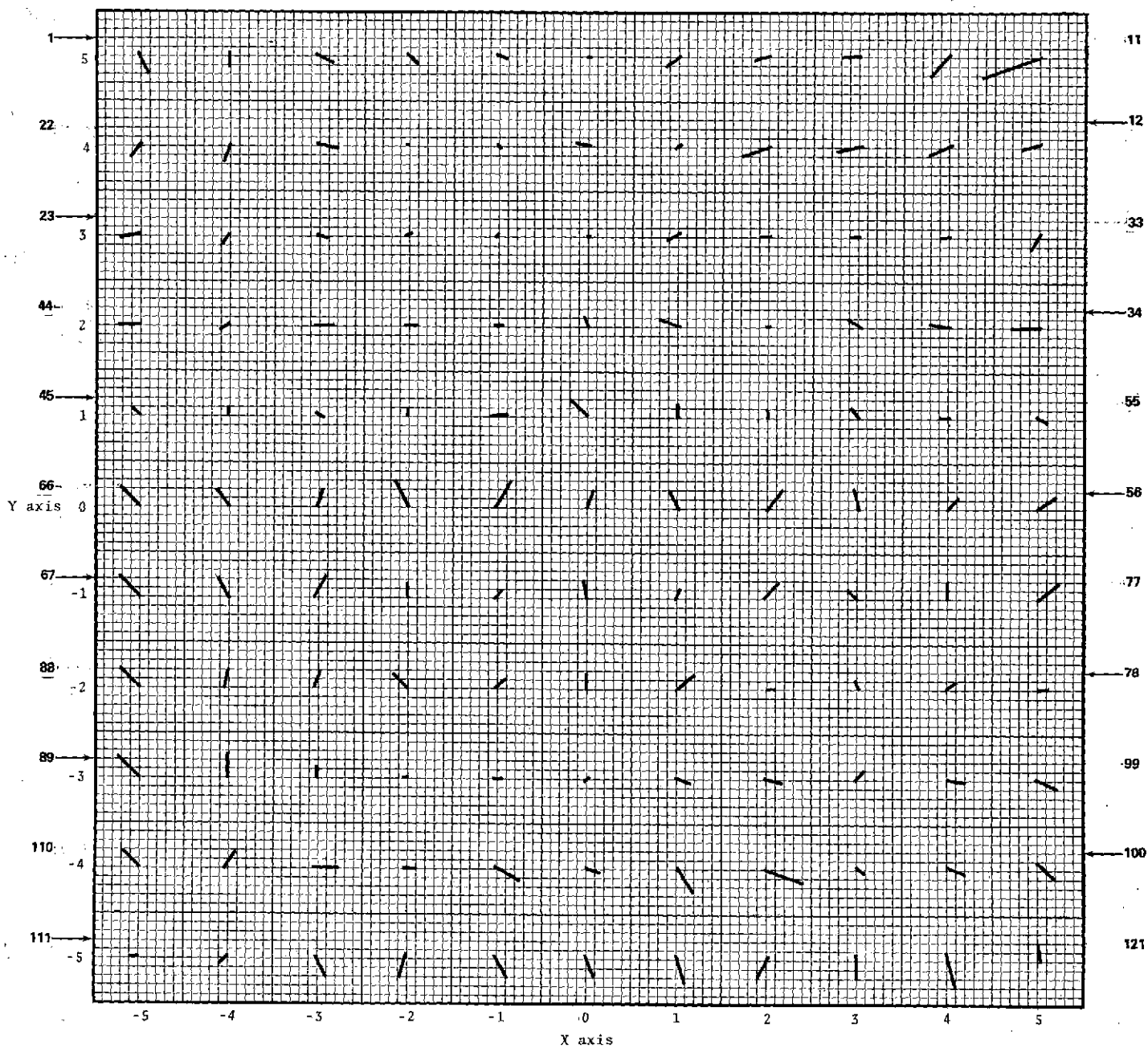


Figure 5. - Sample 121-point field map.



TABLE IV. -- FIELD MAP TEST DATA  
Deviation (Sec)

Data Point	X	Y	Data Point	X	Y
1	11.7	(27.8)	62	19.2	22.8
2	(2.5)	(16.6)	63	(10.4)	30.8
3	21.2	(12.3)	64	7.6	21.4
4	10.9	(13.8)	65	(11.7)	20.0
5	14.3	(6.9)	66	(22.2)	25.7
6	5.5	(0.7)	67	(23.2)	23.2
7	(16.5)	(11.2)	68	(9.9)	24.2
8	(20.4)	(9.1)	69	12.6	26.4
9	(23.1)	(4.0)	70	1.0	14.5
10	(23.8)	(28.3)	71	7.8	6.6
11	(78.8)	(31.1)	72	(0.2)	18.1
12	(26.1)	(4.8)	73	4.8	11.6
13	(28.7)	(14.9)	74	13.5	15.5
14	(31.3)	(10.5)	75	(9.6)	9.1
15	(35.0)	(14.1)	76	1.6	19.6
16	(6.6)	(6.2)	77	26.7	17.4
17	(15.5)	3.5	78	14.9	4.0
18	5.0	(5.1)	79	12.3	5.5
19	1.7	(2.3)	80	(3.1)	11.6
20	25.1	(9.1)	81	9.9	(2.8)
21	(7.8)	(22.4)	82	22.3	14.1
22	(15.2)	(18.5)	83	1.9	16.6
23	(26.1)	(5.5)	84	13.5	8.4
24	(8.5)	(12.4)	85	(15.4)	17.0
25	14.4	(5.9)	86	8.0	17.4
26	7.4	5.3	87	3.6	22.4
27	3.9	6.7	88	(21.1)	21.7
28	(1.7)	2.0	89	(25.0)	22.0
29	(17.6)	(8.4)	90	0.8	26.7
30	(8.9)	(3.7)	91	(0.9)	13.4
31	(12.4)	2.0	92	(4.4)	0.4
32	(16.6)	(5.2)	93	9.6	(0.3)
33	(11.8)	(22.5)	94	(3.5)	(8.3)
34	(26.1)	(5.2)	95	16.6	(9.3)
35	(28.0)	4.2	96	23.1	(9.3)
36	(13.8)	8.9	97	7.9	4.7
37	1.0	2.4	98	19.8	(5.0)
38	(21.9)	8.5	99	23.4	(12.6)
39	(0.2)	11.0	100	19.9	(15.1)
40	6.4	(1.6)	101	23.3	(9.4)
41	14.2	1.6	102	9.7	(7.9)
42	22.2	2.7	103	41.7	(19.5)
43	(13.1)	(5.6)	104	19.8	(33.9)
44	(25.0)	(1.6)	105	15.8	(11.5)
45	(10.0)	9.5	106	30.7	(18.4)
46	(1.7)	7.7	107	14.2	(1.8)
47	11.2	(5.2)	108	29.0	0.4
48	1.3	6.3	109	15.7	21.6
49	14.6	4.9	110	(18.2)	18.7
50	(10.5)	19.6	111		
51	2.4	13.9	112	(9.6)	(13.7)
52	2.1	7.0	113	10.1	(27.8)
53	(4.9)	11.7	114	(6.5)	(31.0)
54	(10.2)	(1.6)	115	17.5	(31.0)
55	8.8	(6.7)	116	8.3	(27.4)
56	21.7	12.0	117	10.5	(34.6)
57	14.4	12.4	118	15.7	(26.3)
58	(4.2)	23.6	119	1.5	(27.4)
59	16.4	17.4	120	6.2	(42.9)
60	(9.1)	15.6	121	3.5	(17.3)
61	8.3	16.7			

ORIGINAL PAGE IS  
OF POOR QUALITY

## 5.0 CONCLUSIONS

The results and data obtained from this evaluation test series produced a number of significant conclusions which were ultimately used in preparation of specifications leading to the procurement of the Orbiter Star Tracker.

### 5.1 Specific Conclusions

5.1.1 Operational test (par 4.1). The test operation successfully showed the capability of the MMOS-B to permit the checking of its modes of operation. Sequencing of modes with operational status signals received from the unit demonstrated the automatic features of the device, as well as its ability to be controlled from an external calculator system. Test experience provided a significant background of information for preparation of specifications for the Orbiter Star Tracker. In particular, the large number of discrete lines associated with the command and status signals offered a good argument for the serial-digital interface selection for the flight model.

5.1.2 Target sensitivity (par 4.2). The MMOS-B was capable of acquiring and tracking a star target of +3 visual magnitude during the test. Since the ultimate sensitivity of the tracker is determined largely by the lens aperture, it was very important to confirm the sensitivity. With this established by the test data, the size, shape, and volume of the flight tracker with its lightshade could be specified with confidence. In fact, the envelope specified was also used as a basis for structural design of the Orbiter Star Tracker compartment.

5.1.3 Target brightness range (par 4.3). The ability of the MMOS-B to acquire track star targets of varying brightnesses from +3 to -3.0 visual magnitude was proved by this test. However, in the test data it was shown that a target position shift appeared when the optical attenuator, located between the lens and photocathode, was actuated. Therefore, the test results indicate that in subsequent designs the method of providing dynamic range adjustments by this means should be improved or changed to prevent excessive target position errors. The Orbiter Star Tracker specifications reflect the concern for this problem by requiring accurate performance throughout the operational dynamic range.

5.1.4 Tracking rate (par 4.4). During the test program a method was developed to measure the angular rate lag error with adequate precision. Consequently, the data was available to substantiate the requirement to include this item in the Orbiter Star Tracker specification. The MMOS-B has a dynamic tracking lag which permits target position bias errors to be as large as one arc minute at angular rates of 0.2 degree per second. The unit also displayed a capability of maintaining track at higher rates up to 0.5 degree per second although target pointing errors exceeded one arc minute.

5.1.5 Magnetic field susceptibility (par 4.5). Image dissector tube trackers are particularly sensitive to magnetic fields unless adequate magnetic shielding is provided in the design. The MMOS-B had been designed to operate in the earth's magnetic field. The results of this

test indicated that the shielding design is adequate to permit operation in the earth's magnetic field with a superimposed magnetic field produced by the passage of a large current through a nearby electrical conductor. Observed operation was without deleterious effect up to the current values achieved. Again, the test offers a base point for establishment of the external magnetic field interference specification of the Orbiter Star Tracker.

5.1.6 False target recognition and rejection test (par 4.6). False target acquisition received a great deal of attention during the preparation of the Orbiter Star Tracker specification because of operational problems with the Apollo Telescope Mount Tracker on Skylab. While there is no safeguard against such problems in the Orbiter Star Tracker design, the test showed that it was possible to provide an onboard software technique for identifying spurious targets and rejecting them in favor of the desired star target. Such spurious targets may be present around the operational Orbiter from sunlit paint particles or ice crystals and could cause the Star Tracker to produce erratic data. This test presents one possible way to avoid the problem by utilizing and controlling the versatile modes to be present in the developed Star Tracker.

5.1.7 Photocathode uniformity (par 4.7). The uniformity of image dissector photocathodes is extremely important to the adequate performance of any using Star Tracker. Data from the test indicated that the tube in the MMOS-B was non-uniform and would not be acceptable in a flight model unit.

Procurement specifications for tubes to be used in the Orbiter Star Tracker should require uniformity patterns of the sensor photocathode which would insure that the surface sensitivity is adequate for the acquisition and tracking of a +3 visual magnitude star target anywhere in the field. In the case of the MMOS-B this could not be due to a 1.2 visual magnitude spread from the least to most sensitive portions. Acceptance tests of the completed unit should be made with photocathode uniformity data available for reference so that tests can be made for minimum operational capabilities at the least sensitive point in the field.

5.1.8 Automatic field map (par 4.8). The automatic field map system used with the MMOS-B was only possible because of the features in the device permitting mode selection from external commands and the supplying of reverse status data to the controlling element. Field map plotting without this method is a laborious and tedious operation requiring extreme caution in adjustment and data collection. The entire operation for a 121-point map (one-degree intervals) can take two operators from 30 to 45 minutes. Since the thermal drift and field skew which occurs during warm-up and subsequent temperature changes has a time duration of one-half to two hours, the manual method cannot be used without serious compromises on its coverage. The automatic method reduces the time to about 2 to 3 minutes for the complete data taking process using the desk calculator method. Therefore, meaningful test data can be taken while the unit is undergoing temperature and other environmental changes, making it possible to analyze the time-dependence of these important error sources.